Scientific Inquiry and Review (SIR)
Volume 9 Issue 1, 2025
ISSN$_{(P)}$: 2521-2427, ISSN$_{(E)}$: 2521-2435
Homepage: https://journals.umt.edu.pk/index.php/SIR

Article QR

Title: **Synthesis and Characterization of Highly Crystalline Strontium Metal-Organic Frameworks using 1,4-Benzenedicarboxylic Acid (BDC) Organic Linker**

Author (s): Rashid Mehmood[1], Ezaz Gilani[1,2], Muhammad Ahmed[1], Momina Feroz[1], and Muhammad Tayyab Saeed[2]

Affiliation (s): [1]Minhaj University, Lahore, Pakistan
[2]University of Engineering & Technology, Lahore, Pakistan

DOI: https://doi.org/10.32350/sir.91.01

History: Received: November 09, 2023, Revised: May 08, 2024, Accepted: January 10, 2025, Published: June 15, 2025

Citation: Mehmood R, Gilani E, Ahmed M, Feroz M, Saeed MT. Synthesis and characterization of highly crystalline strontium metal-organic frameworks using 1,4-Benzenedicarboxylic Acid (BDC) organic linker. *Sci Inq Rev.* 2025;9(1):1–17. https://doi.org/10.32350/sir.91.01

Conflict of Interest: Author(s) declared no conflict of interest

A publication of
The School of Science
University of Management and Technology, Lahore, Pakistan

Synthesis and Characterization of Highly Crystalline Strontium Metal-Organic Frameworks using 1,4-Benzenedicarboxylic Acid (BDC) Organic Linker

Rashid Mehmood[1], Ezaz Gilani[1,2], Muhammad Ahmed[1*], Momina Feroz[1], and Muhammad Tayyab Saeed[2]

[1]Minhaj University, Lahore, Pakistan
[2]University of Engineering & Technology, Lahore, Pakistan

ABSTRACT

In this work, strontium Metal Organic Framework (MOF) using 1,4-benzenedicarboxylic acid (BDC) as the organic linker has been synthesized and characterized. Several industries, such as catalysis, gas storage, and medicinal delivery, have shown interest in strontium metal-organic frameworks (MOFs). Synthesis involves a solvothermal procedure where a controlled reaction environment in which strontium ions are coordinated with BDC ligands, leads to the creation of porous crystalline MOF structures. Various analytical methods were used to characterize the synthesized Sr-MOF. These methods included X-ray diffraction (XRD), scanning electron microscopy (SEM), and Fourier-transform infrared spectroscopy (FTIR), and electron dispersive X-ray spectroscopy (EDX). Strontium metal-organic frameworks with different structural characteristics have been successfully formed, as evidenced by the characterization results. Also, learning about the solvents employed for reaction requirements. By expanding our understanding of Sr-MOF materials and their properties, this study paves the way for future investigations in materials science and chemistry.

Keywords: strontium metal, 1,4-benzendicarboxylic acid (BDC), Metal-organic frameworks. Ligand, Organic Linker.

1. INTRODUCTION

The crystallinity of metal-organic frameworks (MOFs) may be controlled, and their composition and porosity can be adjusted to suit specific needs. It is possible to modify MOFs to have certain features by using a combination of metals and specially designed linkers. Some synthetic techniques for thermally treating MOF precursors to functional

*Corresponding Author: ahmad.ce@mul.edu.pk

materials include pyrolysis, chemical vapour deposition, electrospinning, impregnation, and MOF-templated procedures

[1]. With the numerous applications of MOF, Zinc air batteries (ZABs)O are among the several energy storage devices that have investigated MOFs as a promising material class. They have improved electrocatalytic activity because to more exposed catalytic sites and better transportation made possible by their ordered structure and large surface area, two compositional features. Incorporating other heteroatoms, such as N, S, O, and P, into MOFs can also alter their electrical structure [2]. In the super capacitors, There are primarily two types of super capacitor (SC) applications that have sparked a lot of interest in the use of MOFs in recent years. There are two main applications for metal-organic frameworks (MOFs): the first is as electrode materials, and the second is as templates for various materials, including porous carbons, metal nanoparticles, mixed metal oxides, and metal oxides [3]. Metal sulfides, carbon-based materials with adjustable structures, increased surface area, and diverse chemical compositions, as well as binary metal oxides and double-layered hydroxides, may be efficiently synthesized using precursors based on metal organic frameworks (MOFs). So, it is possible to build binary metal sulfide compounds starting with the preparation of metal oxides or hydroxides by conducting an anion exchange reaction on precursors based on MOFs that have new morphologies and compositions that may be adjusted [4].

Specifically, nitrites (NO2-) and nitrates (NO3-) are two important contaminants in wastewater that are generated as a result of several industrial activities. Although nitrogen oxyanions are not easily recyclable, they can be used as a source to make NH3, which is both valuable and easy to recycle. The toxicity of nitrate is primarily due to nitrite, even though there is more nitrate in wastewater. This is because nitrates can be easily reduced to nitrites in the body. In the gastrointestinal tract, nitrites react with amines and amides to produce carcinogenic N-nitroso compounds. The fact that nitrite is more soluble in water and has a low dissociation energy for N=O bonds causes eNO2RR, or electrocatalytic nitrite reduction, is a potential method for the practical application of MOFs [5]. The redox characteristics, large surface area, and high porosity of MOFs have led to their widespread use in energy storage devices including rechargeable batteries and supercapacitors, as well as in

sensors, photovoltaics, and catalysis. Exploring the use of metal-organic frameworks (MOFs) and materials generated from MOFs as electrodes in the development of high-performance non-Li batteries is a viable and appealing alternative, as are other parts connected to batteries [6]. In heterogeneous catalysis, metal-organic frameworks (MOFs) with distributed monoatomic active sites demonstrate exceptional quasi-molecular catalytic activity. These frameworks are periodic networks that include organic ligands as linkers and metal ions or clusters as nodes [7].

Metal-organic frameworks are the combination of organic-inorganic linker channels resulting in a continuous grid of metal atoms surrounded by organic 'ligand - binding' molecules [8]. The metals create knobs that link the ligand's chains to form a cage structure. Due to their porous nature, MOFs also have greater surface area [9]. Researchers recently have developed metal-organic frameworks consisting of a surface area of considerably well over 7800 m^2 per gram [10]. To summarize, a tablespoon of these MOFs (about 1g of material) could take on a wide soccer field. Metal-organic frameworks show a great variety of structures in comparison to other nano-pores, including homogeneity in architectures, atomic or molecular structural consistency, and efficient permeable ability [11]. A wide range of variability, and diversity in network, geometry, size, and greater usefulness. This made researchers successfully manipulate structure, pore size, and framework functioning [12].

By synthesizing a metal-organic framework that contains different metallic ions & linkers, researchers may produce substances that absorb specific gases into custom-built pores inside the structure. As a result, MOF provides a variety of sensor applications. Similar to Lego bricks, MOF can be arranged in a certain way and show better performance in terms of accessibility to any other class of compounds [13]. Activated carbon, porous carbon formed from metal-organic frameworks (MOFs), carbon nanotubes, aerogels, and other carbon-related materials store energy through the EDLC process [14]. Zeolitic imidazolate framework 8 (ZIF-8) uses the "sieving effect" of a six-membered (6-M) window to effectively separate C3H6 and C3H8. Our results show that ZIF-8 is a flexible material with the potential to efficiently segregate C2H4 and C2H6 through its 4-M window in the <100> direction [15].

Composites with different ratios of PANI and ZrBTB−SO3 are synthesized by using a two-dimensional (2D) zirconium-based metal-organic framework (MOF) with enriched sulfonate-based ligands postsynthetically coordinated onto its nodes as a dispersant during the in situ polymerization of aniline. The composite's PANI may attain a specific capacitance of 515 F/g with the aid of the negatively charged sulfonatefunctionalized 2D MOF sheets used as the dispersant. under conditions of a charge-discharge current of 0.5 mA/cm2, significantly surpassing the results obtained by the pure PANI (230 F/g), PANI@ZrBTB (137 F/g), and the physical combination of PANI and ZrBTB−SO3 (130 F/g) [16].

In some cases, when guest molecules like solvents are evaporated, the voids remain stable and can be interchanged with complex molecules [17]. Through this characteristic, meta-organic frameworks are useful for storing gases like carbon dioxide (CO_2) as well as hydrogen (H_2). They can be used in a range of applications such as gas isolation, sensing, catalysis, conductive solids water treatment, and superconductors [18]. The production and characteristics of metal-organic frameworks are the main concern of a subject called “Reticular-Chemistry” (In Latin word reticulum means "small net"). These MOFs are covalent organic frameworks which were made of small atoms like (B, O, N, H, C) and also have extended structures [19].

The composition and properties of metal-organic frameworks are determined by the metal and the organic ligand used. The number and size of pores are determined by central metal ions, which decide why a large number of ligands may connect to it and from which direction [20].

Numerous metal-organic frameworks have been synthesized including Sr-MOF. The novelty in this research is the Sr with benzene dicarboxylic acid linker shows an amazing porous structure. The graph given under shows the various MOFs along with metal and linkers.

Table 1. The Synthesis of MOF by Various Researchers

No	MOF	Metal	Linker	Ref
1	Magnetic- MOF	Fe_3O_4	UiO-66-NH_2	[21]
2	Cu-MOF	Cu	Graphene oxide	[22]
3	Fe(III)-MOF	Fe	Fe_3-μ_3-oxo clusters	[23]
4	Co-MOF	Co	1,4-benzenedicarboxylate	[24]

No	MOF	Metal	Linker	Ref
5	Li-MOF	Li	napthalenedicarboxylate	[25]
6	Zn-MOF	Zn	$(adb)_2(dabco)$	[26]

2. METHODOLOGY

All the equipment and apparatuses used in synthesis were of fine quality and were in excellent working condition. The glassware used while experimentation were beakers, measuring cylinders, a burette, an hot plate, a magnetic stirrer by VELP SCIENTIFICA, electronic weight balance by SHIMADZU JAPAN, and a thermostatic drying oven by SANFA.

The organic linker used was 1,4-Benzenedicarboxylic Acid by Sigma-Aldrich, Dimethyl Formamide(DMF) was taken as a solvent, and other organic solvents like Dimethyl sulphoxide(DMSO) and other chemicals including metal salt (Strontium chloride) etc were provided & arranged by MINHAJ UNIVERSITY LAHORE.

In this crystalline metal-organic framework, $SrCl_2$ acta as a metal cation while electron-donating species like 1,4-Benzenedicarboxylic act as a ligand.

Preparation of salt solution: For the preparation of 0.1M salt solution, 0.5 gram SrCl2 was weighed using an electronic weighing balance. The solubility of salt in different organic solvents such as DMF and DMSO was checked as well. SrCl2 showed a great extent of solubility towards DMSO. So prepared the 30-50 ml of SrCl2 solution in a two-neck flask and labeled it as solution “A”

All the glass apparatus was rinsed with distilled water, weighted 0.5g of 1,4-Benzenedicarboxylic Acid, and made soluble solution in DMF/DMSO then poured 30 to 50 ml of it into a burette (VIPR sigma) already set along its stand.

2.1. Procedure

Step-wise detailed experimental summary as explained below:

Place solution “A” on a Hot plate magnetic stirrer (VELP SCIENTIFICA) and set the burette to stand so that the drops of burette smoothly run into the solution “A”. The mixing speed must be very low to control the size. Controlled reaction conditions were maintained in

throughout the entire process as the temperature was kept at 30-35°C and stirring speed kept moderate.

When 15 to 20% (0.1M 1,4-Benzenedicarboxylic Acid) was utilized, the color of the reaction mixture changed from white to greenish which ensured that the reaction was going in the right direction. At the ending stage, when 30 ml-40 ml of the (0.1M 1,4-Benzenedicarboxylic Acid) was consumed, some white cloudiness appeared in the flask.

After complete mixing of metal salt & organic linker, keep the mixture on stirring for a further 2 to 3 hours. Then to carry out our complete reaction the mixture was sent in solvothermal and kept in the oven at 120^0C for 12 hr. After 12 hours transferred it into a beaker and allowed crystals to settle down properly. For recrystallization, evaporate the excess solvent present in it by heating it to get more fine crystals of prepared MOF. The crystals were dried in the drying oven for 3-4 hours at 60^0C. After those crystals were cooled at room temperature for an hour. In the end, the sample was stored in air-free clean dry sample vials.

3. RESULTS& DISCUSSION

The sample was analyzed by three characterization techniques. To elucidate different functional groups in the newly synthesized metal-organic frameworks FT-IR (Fourier-Transform Infrared spectroscopy) was done. To read the surface morphology of the product SEM (Scanning electron microscopy) was done while the crystalline structure of MOF was determined by XRD (X-ray diffraction) analysis. Experiments were conducted by following standard methods proposed with bit modifications.

3.1. SCANNING ELECTRON MICROSCOPIC (SEM) ANALYSIS

To illustrate the morphology and synthesis of the Sr-MOF, we used scanning electron microscopic technique. The lower and higher amplified SEM pictures of products are shown in Figure 1. The Fig shows the sample (Sr-MOF) Nanosheets having length and width with ranges in 130.8-145.5 µm and 132.6-140.2 µm, separately and they have thickness around 28 ± 9 µm. Figure 2 shows that the Sr-MOF has a porous structure with uneven particle size.

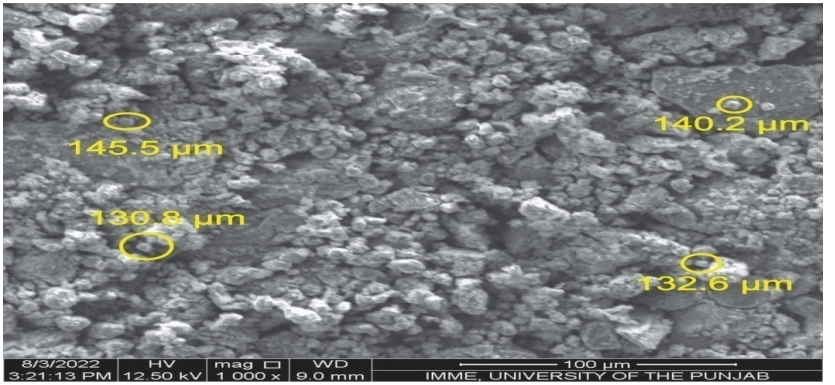

Figure1. Surface Particle Arrangement on Sr-MOF by SEM

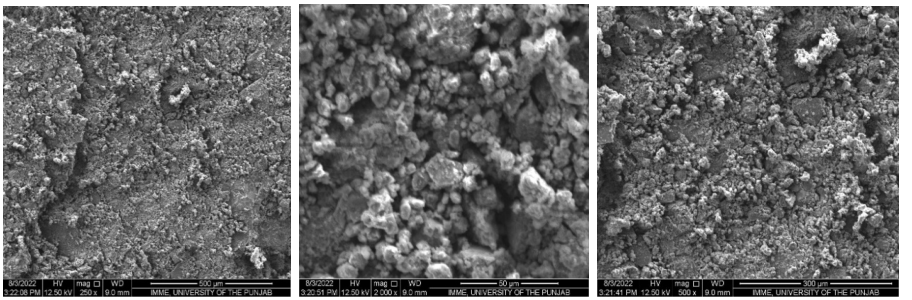

Figure 2. (a)(b)(c) Morphology of Sr-MOF by SEM

3.2. Energy Dispersive X-RAY Spectroscopy

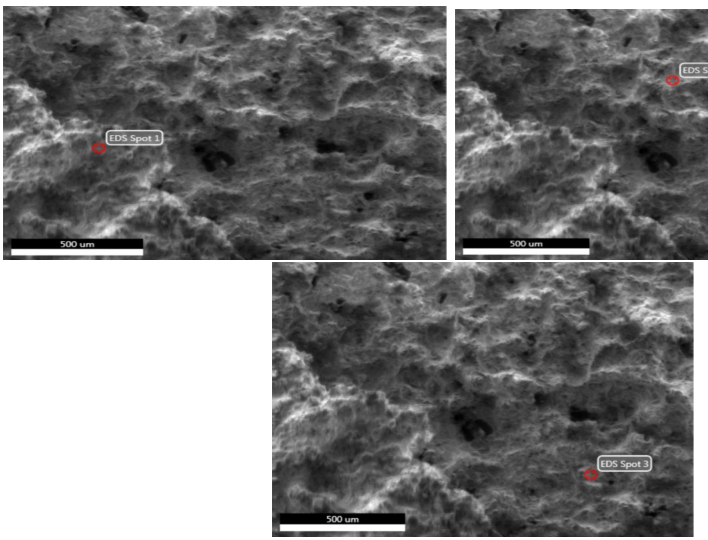

Figure 3. (a)(b)(c) The EDX Results of Sr-MOF

To determine the conformity of formation of Sr-MOF the EDX spectroscopy was performed. Several areas were focused on different sites which confirmed the formation of Sr-MOF. Spectrum Fig 3(a) illustrated the quantity of O, Sr, and Cl were 37.47, 19.28, and 43.26 measured in atomic % respectively. Similarly, Fig.2(b) depicted the quantity of O, Sr, and Cl were 34.36, 21.13, and 44.51 determined in atomic % respectively. The overall result is shown in the table.

Table 2. The Various Result Obtained by EDX of Sr-MOF

Sr-MOF	Oxygen (O)		Strontium (Sr)		Chlorine (Cl)	
	Weight (%)	Atomic (%)	Weight (%)	Atomic (%)	Weight (%)	Atomic (%)
Sample(a)	15.68	37.47	44.19	19.28	40.12	43.26
Sample(b)	13.82	34.36	46.52	21.13	39.66	44.51
Sample(c)	23.07	48.9	39.48	15.28	37.45	35.82

3.3. Fourier Transform Infrared (FT-IR) Spectroscopy

FT-IR gives information about organic functional groups. FT-IR spectra of Sr-MOF are shown in Fig. 3. The Sr-based MOFs carbonyl groups stretching appeared at 1671 cm^{-1} respectively. The characteristic broad peak of OH stretching is at 3390.35 cm^{-1} while peaks in region 3062-3102 is of aromatic C=C-H and the peaks between 1420.70-1572.11cm^{-1} are of aromatic C=C-C. Peaks at 1278.67cm-1 indicate the C-O-C functional group. Frequencies between 878-925cm^{-1} are of 1,4 di-substitution on the benzene ring. Sr metal has been coordinated to the oxygen of ligand is confirmed by the presence of a peak at 778.18cm^{-1}. There are several of cases where the Sr based compounds such as strontium ferrite give the FTIR peak between 700-800 cm^{-1}[27].

Table 3. FT-IR Spectroscopy

Wave Number(cm^{-1})	Functional Group
3390.35	OH Streching
1671.00	C = O
3062-3102	Aromatic ring C=C-H
1420.70-1572.11	Aromatic C=C-C
1278.67	C-O-C
878.33-925.51	Ortho and para position substituted
778.18	Sr-O

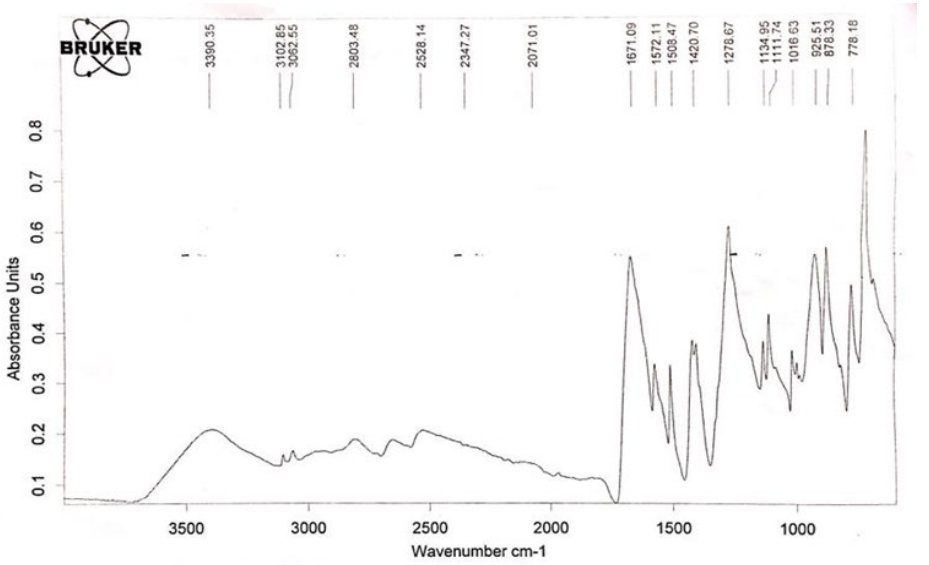

Figure 4. FT-IR of Sr-MOF

3.4. XRD Analytical Result

The following significant diffraction angles were confirmed by the powder XRD (XRD) technique that the diffraction pinnacles of the item well coordinated with hexagonal SrO.

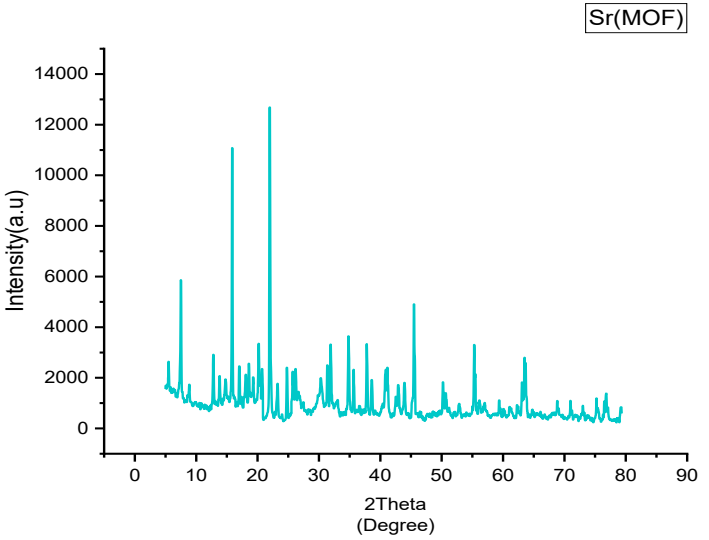

Figure 5. Graphical Representation of Sr-MOF through XRD Analysis

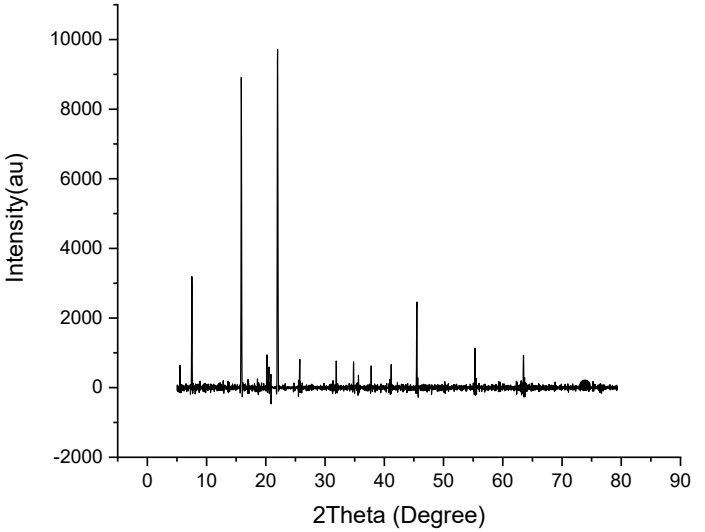

.

Figure 6. XRD of Sr-MOF Graph with Baseline Correction

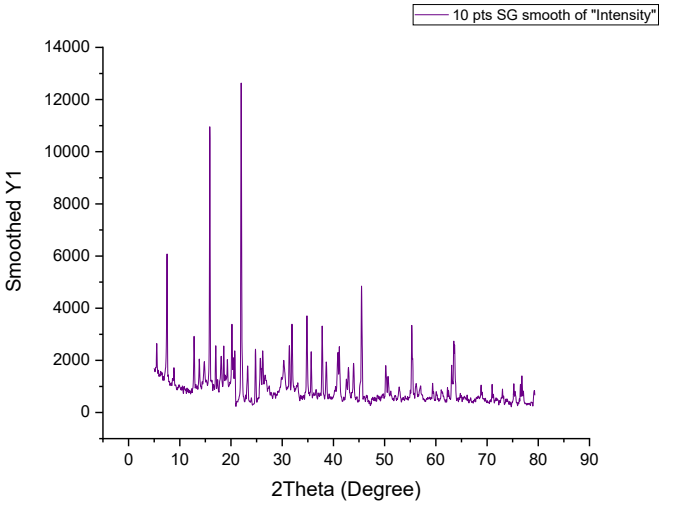

Figure 7. XRD of Sr-MOF graph smoothed by 10 pts

3.4.1. Crystal Size. Crystallite sizes from X-ray diffraction graphs were determined with the use of the origin (software) program. Full-width half maximum (FWHM) is used in X-ray Diffraction to quantify the size of crystallites. Halfway between the peak maximum and the background, the width of the diffraction peak (in radians) is known as the full width at

half maximum (FWHM). Scherrer's equation is used to calculate the Nano crystallite size (D) of X-ray Diffraction radiation with wavelength (nm) by measuring the full width at half maximum (FWHM) of peaks in radians at any 2 in the pattern. This formula applies to crystallite sizes up to around 200 nm.

$$\mathbf{D=K\lambda/\beta\cos\theta}$$

D = Crystallite size (nm)

K= Scherrer constant, the value of K is 0.94.

λ = X-ray wavelength= 1.5406Å

θ= Bragg's angle in degree, half of 2θ

β= line broadening at FWHM in radians

Although the strongest peak in the XRD pattern is often employed as a proxy for crystallite size, this approach is often inaccurate. To calculate the average crystallite size (D average), data from all peaks are added together. The Scherrer constant (K) is always 0.94 for cubic crystals. D and the Scherrer constant have been shown to have a one-to-one relationship.

Table 4. The Crystalline Size of Sr-MOF

K	Λ	2θ	FWHM (β)	Crytallite size D nm
0.94	1.5406	21.994	0.161	52.5

3.4.2. Percentage Crystallininty. The crystallinity of the Sr-MOF sample was measured using XRD data by determining the area of each crystalline peak and the overall area (crystalline and amorphous).

$$\%\ \mathbf{Crystallinity} = \mathbf{Area\ of\ all\ crystalline\ peaks/TotalArea\times 100}$$

$$\%\ \mathbf{Crystallinity} = 44317.78/73840.25 \times 100$$

$$\%\ \mathbf{Crystallinity} = 60.01\%$$

3.4.3. D-Spacing. D-spacing, also known as interplanar spacing, is the distance between two successive atomic planes. It can be used to determine the composition or structure of crystals. Based on the angle of diffraction, the difference between atomic planes can be computed using Bragg's law. The d-spacing is computed by applying Bragg's equation.

$$n\lambda = 2dSin\theta$$

$$d = n\lambda / 2Sin\theta$$

Table 5. The Interplanar Spaces between Two Successive Atomic Planes

2Theta	Theta	D-spacing
7.50736	3.75368	5.895745
15.8909	7.94545	2.813301
21.99401	10.99701	2.056823
45.5097	22.75485	1.079806
55.33879	27.6694	0.936502
62.41706	31.20853	0.869078
40.98958	20.49479	1.174378
37.81257	18.90629	1.256442
34.83621	17.41811	1.348488
31.44613	15.72307	1.476528
20.30917	10.15459	2.219336
15.8909	7.94545	2.813301
5.579	2.7895	7.92342

4. CONCLUSION

The manufacturing of Sr-MOF in solvothermal conditions enable us to generate a novel porous compound strengthening the material science and his application has a marvelous effect on various applications related to Sr-MOF. The synthesis of Sr-MOF has been made possible by refluxing 1-4 benzene dicarboxylic acid with the salt of strontium metal in ratio 1;1, the structural characteristics of Sr-MOF were determined by three characterization techniques as FTIR, XRD, EDX and SEM. Scanning electron microscopy (SEM) suggests that the surface morphology of Sr-MOF has a porous structure with uneven particle size. X-ray Diffraction technique (XRD) gives information about the percentage crystallinity of Sr-MOF which came out around 60.01% and crystallite size is measured by using Sherrer's equation which is approximately aqual to 52.5nm, while D-spacing is measured by applying Bragg's equation which ranges between 0.8-7.9 overall. The information about functional groups present in Sr-MOF was confirmed by FTIR studies. The peak at 778cm-1 confirms that the ligand is coordinated to metal Sr. The EDX spectroscopy depicted the confirmation of Sr metal present in the MOF with various

amounts. The Sr-MOF can serve in the gas storage, as a catalyst, in the drug delivery system, to detect various molecules or ions in the environment, in gas separation for chemical separation, and in the energy storage devices.

CONFLICT OF INTEREST

The authors of the manuscript have no financial or non-financial conflict of interest in the subject matter or materials discussed in this manuscript.

DATA AVALIABILITY STATEMENT

The data associated with this study will be provided by the corresponding author upon request.

FUNDING DETAILS

No funding has been received for this research.

REFERENCES

1. Prinz N, Strübbe S, Bauer M, Zobel M. Structural transitions during Ni nanoparticle formation by decomposition of a Ni-containing metal–organic framework using in situ total scattering. *New J Chem*. 2023;47(24):11623–11635. https://doi.org/10.1039/D3NJ00493G
2. Devi B, Kurungot S. Conductive metal-organic frameworks for zinc-air battery application: design principles, recent trends and prospects. *J Mater Chem A*. 2024;12(5):2605–2619 https://doi.org/10.1039/D3TA03753C
3. Adil M, Olabi AG, Abdelkareem MA, et al. In-situ grown metal-organic framework derived CoS-MXene pseudocapacitive asymmetric supercapacitors. *J Energy Storage*. 2023;60:e106537. https://doi.org/10.1016/j.est.2022.106537
4. Saeed G, Alam A, Bandyopadhyay P, Jeong S, Kim K, Lim S. Metal-organic framework-derived (Mn-1) CoxSy@(Ni–Cu) OHs marigold flower-like core@ shell as cathode and (Mn–Fe10) Sx@ graphene–foam as anode materials for ultra-high energy-density asymmetric supercapacitor. *Mater Today Chem*. 2022;23:e100758. https://doi.org/10.1016/j.mtchem.2021.100758

5. Ghatak A, Shanker GS, Sappati S, Liberman I, Shimoni R, Hod I. Pendant proton-relays systematically tune the rate and selectivity of electrocatalytic ammonia generation in a fe-porphyrin based metal-organic framework. *Angew Chem, Int Ed*. 2024:e202407667. https://doi.org/10.1002/anie.202407667

6. Thakur AK, Majumder M, Patole SP, Zaghib K, Reddy M. Metal–organic framework-based materials: advances, exploits, and challenges in promoting post Li-ion battery technologies. *Mater Adv*. 2021;2(8):2457–2482. https://doi.org/10.1039/D0MA01019G

7. Feng D, Zhou L, White TJ, Cheetham AK, Ma T, Wei F. Nanoengineering metal–organic frameworks and derivatives for electrosynthesis of ammonia. *Nano-Micro Lett*. 2023;15(1):e203. https://doi.org/10.1007/s40820-023-01169-4

8. Kalaj M, Bentz KC, Ayala Jr S, et al. MOF-polymer hybrid materials: From simple composites to tailored architectures. *Chem Rev*. 2020;120(16):8267–8302. https://doi.org/10.1021/acs.chemrev.9b00575

9. Zhang X, Wan K, Subramanian P, Xu M, Luo J, Fransaer J. Electrochemical deposition of metal–organic framework films and their applications. *J Mater Chem A*. 2020;8(16):7569–7587. https://doi.org/10.1039/D0TA00406E

10. Nabipour H, Mozafari M, Hu Y. BioMOFs. In: Mozafari M, ed. *Metal-Organic Frameworks for Biomedical Applications*. Elsevier; 2020:321–345. https://doi.org/10.1016/B978-0-12-816984-1.00017-2

11. Tranchemontagne DJ, Hunt JR, Yaghi OM. Room temperature synthesis of metal-organic frameworks: MOF-5, MOF-74, MOF-177, MOF-199, and IRMOF-0. *Tetrahedron*. 2008;64(36):8553–8557. https://doi.org/10.1016/j.tet.2008.06.036

12. Safaei M, Foroughi MM, Ebrahimpoor N, Jahani S, Omidi A, Khatami M. A review on metal-organic frameworks: synthesis and applications. *TrAC Trends Anal Chem*. 2019;118:401–425. https://doi.org/10.1016/j.trac.2019.06.007

13. Furukawa H, Cordova KE, O'Keeffe M, Yaghi OM. The chemistry and applications of metal-organic frameworks. *Science*. 2013;341(6149):e1230444. https://doi.org/10.1126/science.1230444

14. Pathak I, Acharya D, Chhetri K, et al. Ti 3 C 2 T x MXene embedded metal–organic framework-based porous electrospun carbon nanofibers as a freestanding electrode for supercapacitors. *J Mater Chem A*. 2023;11(10):5001–5014. https://doi.org/10.1039/D2TA09726E

15. Wei R, Liu X, Zhou Z, et al. Carbon nanotube supported oriented metal organic framework membrane for effective ethylene/ethane separation. *Sci Adv*. 2022;8(7):eabm6741. https://doi.org/10.1126/sciadv.abm6741

16. Tsai M-D, Chen Y-L, Chang J-W, Yang S-C, Kung C-W. Sulfonate-functionalized two-dimensional metal–organic framework as a "dispersant" for polyaniline to boost its electrochemical capacitive performance. *ACS Appl Energy Mater*. 2023;6(21):11268–11277. https://doi.org/10.1021/acsaem.3c02155

17. Li W. Metal–organic framework membranes: production, modification, and applications. *Prog Mater Sci*. 2019;100:21–63. https://doi.org/10.1016/j.pmatsci.2018.09.003

18. Bai S, Liu X, Zhu K, Wu S, Zhou H. Metal–organic framework-based separator for lithium–sulfur batteries. *Nat Energy*. 2016;1(7):1–6. https://doi.org/10.1038/nenergy.2016.94

19. Lee J, Farha OK, Roberts J, Scheidt KA, Nguyen ST, Hupp JT. Metal–organic framework materials as catalysts. *Chem Soc Rev*. 2009;38(5):1450–1459. https://doi.org/10.1039/B807080F

20. Gangu KK, Maddila S, Mukkamala SB, Jonnalagadda SB. A review on contemporary metal–organic framework materials. *Inorg Chimica Acta*. 2016;446:61–74. https://doi.org/10.1016/j.ica.2016.02.062

21. Yin LL, Kong XY, Zhang Y, Ji YQ. Facile synthesis of the magnetic metal organic framework Fe3O4@ UiO-66-NH2 for separation of strontium. *Biomed Environ Sci*. 2018;31(6):483–488. https://doi.org/10.1016/j.ica.2016.02.062

22. Petit C, Burress J, Bandosz TJ. The synthesis and characterization of copper-based metal–organic framework/graphite oxide composites. *Carbon*. 2011;49(2):563–572. https://doi.org/10.1016/j.carbon.2010.09.059

23. Laurier KG, Vermoortele F, Ameloot R, De Vos DE, Hofkens J, Roeffaers MB. Iron (III)-based metal–organic frameworks as visible light photocatalysts. *J Am Chem Soc*. 2013;135(39):14488–14491. https://doi.org/10.1021/ja405086e

24. Hu X, Hu H, Li C, et al. Cobalt-based metal organic framework with superior lithium anodic performance. *J Solid State Chem*. 2016;242:71–76. https://doi.org/10.1016/j.jssc.2016.07.021

25. Banerjee D, Kim SJ, Parise JB. Lithium based metal− organic framework with exceptional stability. *Cryst Growth Des*. 2009;9(5):2500–2503. https://doi.org/10.1021/cg8014157

26. Hauptvogel IM, Biedermann R, Klein N, et al. Flexible and hydrophobic Zn-based metal–organic framework. *Inorg Chem*. 2011;50(17):8367–8374. https://doi.org/10.1021/ic200937u

27. Tavakolinia F, Yousefi M, Afghahi SSS, Baghshahi S, Samadi S. Synthesis of novel hard/soft ferrite composites particles with improved magnetic properties and exchange coupling. *Proc Appl Ceram*. 2018;12(3):248–256. https://doi.org/10.2298/PAC1803248T